



## The impact of essential climate variables on respiration rates in subpolar and polar planktonic foraminifera

Diane V. Armitage,<sup>1</sup> Nicolaas Glock<sup>2</sup>, Thomas L. Weiss,<sup>1,3</sup> Mohamed M. Ezat,<sup>4</sup> Adele Westgård<sup>4</sup>, Freya Sykes<sup>4</sup>, Julie Meiland<sup>5</sup>, Elwyn de la Vega<sup>1</sup>, Alessio Fabbrini<sup>1</sup>, Tali, L. Babila<sup>6</sup>, Audrey Morley<sup>1,3</sup>

<sup>1</sup>School of Geography, Archaeology, and Irish Studies, and Ryan Institute, University of Galway, Ireland, H91 TK33, Ireland.

<sup>2</sup>Institute for Geology, University of Hamburg, Bundesstraße 55, 20146 Hamburg, Germany

<sup>3</sup>iCRAG – Irish Centre for Research in Applied Geosciences, Belfield, Dublin 4, D04 V1W8, Ireland.

<sup>10</sup><sup>4</sup> iC3: Centre for ice, Cryosphere, Carbon and Climate, Department of Geosciences, UiT - The Arctic University of Norway, 9037 Tromsø, Norway

<sup>5</sup>Aix-Marseille Université, CNRS, IRD, INRAE, CEREGE, Aix-en-Provence, France

<sup>6</sup>Department of Earth, Environmental and Planetary Sciences, Case Western Reserve University, 44106, Cleveland, USA

15

*Correspondence to:* Diane V. Armitage ([D.Armitage1@universityofgalway.ie](mailto:D.Armitage1@universityofgalway.ie)) and Audrey Morley ([audrey.morley@universityofgalway.ie](mailto:audrey.morley@universityofgalway.ie))

**Abstract:** This study investigates the impact of Essential Climate Variables (ECVs) on the respiration rate of polar planktonic foraminifera *Neogloboquadrina pachyderma* and subpolar *Turborotalita quinqueloba* and <sup>20</sup> *Neogloboquadrina incompta* to advance our understanding of foraminifera physiology and geochemical proxy interpretation for species living in understudied subpolar and polar environments. Respiration rates were measured on a total of 166 specimens collected during two field campaigns to the Nordic Seas. To size-normalise respiration rates we measured cavity volume and maximum diameter using x-ray microcomputed tomography (micro-CT) ( $^{3\sqrt{}}\text{cavity volume} = (0.56(\max \varnothing) - 0.38)$ ). Our results show that the physiological response of foraminifera sharing overlapping environments is diverse, with *N. pachyderma* exhibiting remarkable stability over large gradients in temperature, salinity, carbonate chemistry, dissolved oxygen and nutrients. Conversely, *N. incompta* and *T. quinqueloba* have a much stronger thermal response. The difference between species is best described by their respective  $Q_{10}$  (the factor by which the rate of respiration changes with a 10°C increase in temperature) values of 1.41 for *N. pachyderma* and 3.45 and 4.55 for *N. incompta* and *T. quinqueloba*, respectively. We also find a <sup>25</sup> significant relationship between cavity volume and respiration rate ( $\text{Log}_{10} \text{respiration rate} = 0.399 (\text{Log}_{10} \text{cavity volume}) - 5.785$ ) for all three species analysed here, which is consistent with marine protists globally. We conclude that respiration is unlikely to influence geochemical proxies and therefore past climate reconstructions derived from *N. pachyderma*, however, this may not apply to *N. incompta* and *T. quinqueloba*.

### 1. Introduction

<sup>35</sup> Planktonic foraminifera are relatively eurythermal and inhabit a wide range of temperatures and environments while maintaining species-specific temperature preferences (Chabaane et al. 2024). Accordingly, many species can be found across large temperature gradients exceeding 10°C, and yet, studies focussing on temperate and tropical species have found a strong influence of temperature and cell volume on respiration and growth rate indicating a strong influence of changing environments on foraminifera physiology (Rink et al., 1998; Lombard



40 et al., 2009; Burke et al., 2025). However, little is known about how subpolar and polar planktonic foraminifera respiration responds to temperatures below 10°C and other **ECVs** such as salinity, carbonate chemistry, and nutrients. Specifically, there are no observations of the physiological processes underlying the growth and response of these species to environmental stressors such as modern **Arctic** Amplification (the warming of the Arctic at four times the global mean rate) (Serreze and Barry, 2011; Rantanen et al., 2022). Critically, this gap in  
45 our knowledge, limits our understanding of how foraminifera will adapt to rapid environmental change and our ability to predict the future resilience of these ecosystems.

Respiration also significantly influences foraminiferal shell chemistry by modifying the seawater chemistry in the microenvironment surrounding the test (Schiebel and Hemleben, 2017). For example, increased respiration has been shown to alter carbon isotope ( $\delta^{13}\text{C}$ ) values (used in reconstructing past changes in water mass properties or  
50 productivity) (Spero and Lea, 1993, 1996) and Mg/Ca ratios (for inferring past sea surface or bottom water temperatures) (Rink et al., 1998; Köhler-Rink and Kühl, 2001; Eggins et al., 2004). Respiration influences these proxies because  $\text{O}_2$  consumption lowers the pH in the diffusive boundary layer, which in turn alters the carbonate chemistry transported to the site of calcification (Wolf-Gladrow et al., 1998; de Nooijer et al., 2014). This raises concerns about non-thermal factors that may alter foraminiferal geochemistry and affect the reliability of  
55 temperature reconstructions. Investigating how respiration in polar and subpolar species responds to temperature and other ECVs is thus key to evaluating whether such physiological processes may introduce uncertainties into geochemical proxies recorded in their shells.

Within the polar oceans, *Neogloboquadrina pachyderma* is the dominant planktonic foraminifera species (Al-Sabouni et al., 2007; Husum and Hald, 2012; Chaabane et al., 2024), making up more than 90% of the total  
60 assemblages in waters  $<4^\circ\text{C}$  (Spindler, 1996; Greco et al., 2019; Bertlich et al., 2021) and up to 23% of the calcium carbonate  $\text{CaCO}_3$  flux to the sediments north of  $50^\circ$  (Tell et al. 2022). *Neogloboquadrina pachyderma* maintains a unique adaptation to these extremely cold and diverse environments including low temperatures ( $-2$  to  $+12^\circ\text{C}$ ) and large gradients in salinity ( $\sim 30 - 35$  psu) including brine channels with salinities of up to 80 psu, and pH (7.8 - 8.8) (e.g., Spindler and Dieckmann, 1986; Manno et al., 2012; Bertlich et al., 2021; Zamelczyk et al. 2021; Westgård et al., 2023). The closely related foraminiferal species *Neogloboquadrina incompta* typically inhabits subpolar surface waters (relative abundance  $>50\%$ ) where sea surface temperatures (SSTs) range between 10 and  $18^\circ\text{C}$ . The largest abundances of *N. incompta* occur at salinities ranging between 31 and 35 psu (Greco et al., 2020). *Turborotalita quinqueloba* is most abundant in subpolar waters of the West Spitzbergen Current (Volkmann, 2000) and the Barents Sea with recent studies in that area reporting maximum relative abundances of  
65 26% (Meiland et al., 2019; Anglada-Ortiz et al., 2025). Its maximum abundance occurs at a salinity of 35 psu (Natland, 1938).

The objective of this study is to measure the respiration rates of polar (*N. pachyderma*) and sub-polar (*N. incompta* and *T. quinqueloba*) foraminifera to assess the relationship between respiration and ECVs (temperature, salinity, pH, dissolved oxygen, alkalinity, and  $\Omega\text{Ca}$ ), including nutrients (Silicate ( $\text{SiO}_2$ ), Dissolved Inorganic Carbon (DIC), Phosphate ( $\text{PO}_4^{3-}$ ), and Total Organic Nitrogen (TON)) for these species. This will allow us to test the hypothesis that temperature has a direct effect on respiration rates as observed in temperate and tropical species (Lombard et al., 2009). Similarly, we will test the physiological dependence of external pH and carbonate chemistry on respiration rates in non-spinose planktonic foraminifera species, which is hypothesized to be reduced  
75



due to higher energy requirements of calcification under low pH conditions (Davis et al., 2017). Although earlier  
80 research on nutrients such as  $\text{PO}_4^{3-}$  and  $\text{SiO}_2$  found they are not directly utilised by foraminifera, with their primary effects instead arising through impacts on primary productivity (Schiebel et al., 2001), more recent research on benthic foraminifera has found that  $\text{PO}_4^{3-}$  can be accumulated for energy metabolism, pH regulation, and osmoregulation (Glock et al., 2020, 2025), a capacity that may likewise occur in planktonic foraminifera. Including these variables therefore allows us to explore potential indirect effects and assess whether environmental  
85 variability contributes to physiological stress or metabolic shifts which could be demonstrated through changes in respiration. The results will allow us to assess the importance of respiration for polar and subpolar planktonic foraminifera and thereby further our understanding on their ability to adapt to rapid environmental change. In addition, our results will allow us to review the importance and implications of respiration for geochemical proxies measured in these three species.

90 Determining the response of respiration to temperature requires accurate measurements of individual foraminiferal respiration under controlled settings. Recent advancements in micro-sensor periphery technology, particularly the nano-respiration and rosette methodology developed by Unisense (Lopes et al., 2005; Nielsen et al., 2007), have significantly improved the reproducibility required to detect extremely low respiration rates encountered in smaller sized planktonic foraminifera species e.g.  $< 200 \mu\text{m}$  living in polar and subpolar environments. The  
95 automated rosette allows for more repetition due to faster analysis time compared to traditional manual profiling and enhanced throughput which minimises stress on specimens during experimentation. In addition, the precise determination of internal foraminiferal biovolume is required for size normalisation, since cell size may correlate positively with respiration as in both benthic (Hannah et al., 1994; Geslin et al., 2011) and other planktonic foraminifera (Burke et al., 2025). Methods for accurately estimating biovolume vary in the literature, often relying  
100 on geometric approximations (e.g. Hannah et al., 1994; Cesbron et al., 2016; Geslin et al., 2011; Macuite et al., 2023), however, the use of high-resolution micro-CT scanning (Burke et al., 2020) provides a more accurate means to assess internal volume and will enable us to refine the metabolic relationships between size and respiration rate.

## 2. Methods

### 105 2.1. Sample collection and processing

Living specimens of *N. pachyderma*, *N. incompta*, and *T. quinqueloba* analysed in this study were obtained during two oceanographic cruises on the RV Celtic Explorer in July/August 2023 (CE23011) and on the RV Helmer Hansen (ARCLIM-24-1) in June 2024 (Table 1 and Fig. 1). Plankton samples were collected using  $100 \mu\text{m}$  vertical-closing HydroBios multinets and  $63 \mu\text{m}$  vertical-closing WP2 nets, respectively. Seawater samples were  
110 collected with Niskin bottles attached to a CTD profiler and filtered using a vacuum pump with  $0.2 \mu\text{m}$  Whatmann filters Type G/C and refrigerated. Live foraminifera were picked directly from the plankton net samples and transferred into a petri dish for an initial bath to remove debris and algae attached to the foraminifera. For the first set of experiments in 2023, a small brush and a dissecting microscope were used to select and transfer living specimens into culture wells (CE23011), placed in an incubator set to the towed environment of the samples, and  
115 allowed to rest for at least 12 h and no longer than 24 h before respiration rate measurements were performed on board (CE23011). Foraminifera were not fed prior to respiration measurements to be consistent with common

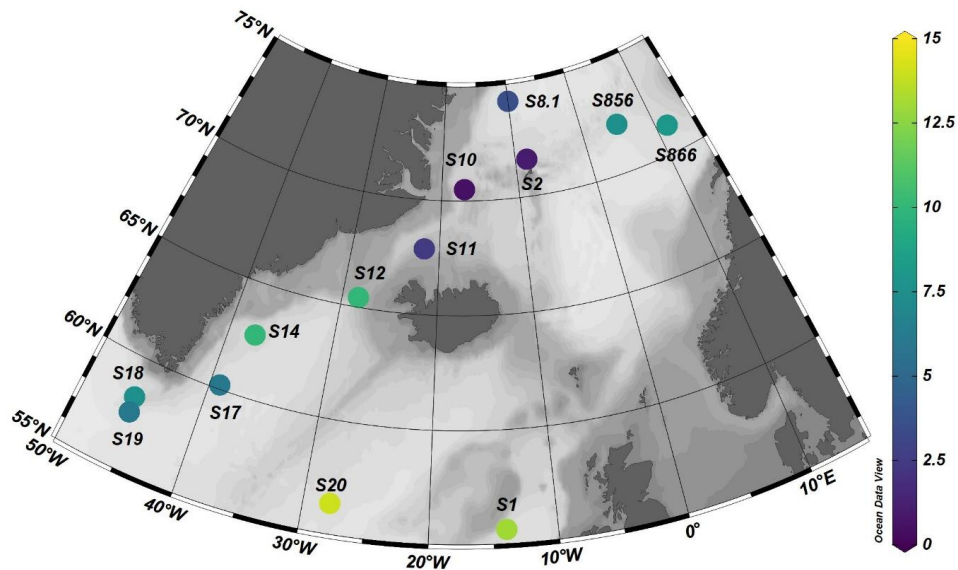


practice on similar planktonic foraminifera respiration studies (Davis 2017; Rink 1998; Burke 2025; Lombard 2009).

120 For the second set of experiments performed in 2024, all collected specimens were transferred from the initial bath into 75 ml culture bottles and placed into a cold room set at 8 °C during the cruise. After the initial 24 h resting period, the foraminifera were fed 40 µL of a live diatom solution, a self-replicating food source (Fabbrini et al., submitted). Subsequently, culture bottles were transferred into incubators set at experimental temperatures of 2 °C, 5 °C, 8 °C and 13 °C for at least 48 h before flux measurements were performed in the Culturing Laboratory at UiT the Arctic University of Norway. An additional feeding of algae (*Nannochloropsis sp.*) took place 7 days 125 after sampling. All experiments in 2024 were carried out within 11 days of sampling.

**Table 1** Metadata, ecological and carbonate chemistry data for analysed samples. NA indicates no data collected at these stations.

Station [ID]	Taxon	Start	End	Lat [N]	Long [E]	Depth [m]	SST [oC]	Sal [psu]	DIC [µmol.kg <sup>-1</sup> ]	Alk	pH
CE23011_1	<i>N. incompta</i>	23/07/2023	24/07/2023	55.64	-14.01	40	13	35.45	2138	2309	7.98
CE23011_2	<i>N. pachyderma</i>	28/07/2023	29/07/2023	71.63	-8.42	50	1	34.58	2156	2276	7.93
CE23011_8.1	<i>N. pachyderma</i>	02/08/2023	04/08/2023	74.25	-10.07	75	3.5	34.92	2172	2300	8.12
CE23011_10	<i>N. pachyderma</i>	04/08/2023	05/08/2023	70.5	-17.09	100	0.5	34.57	2158	2293	8.07
CE23011_11	<i>N. pachyderma</i>	05/08/2023	06/08/2023	67.87	-21.77	125	2.5	34.76	2169	2298	8.06
CE23011_12	<i>N. pachyderma</i>	07/08/2023	08/08/2023	65.42	-28.33	20	10	35.09	2110	2317	8.08
CE23011_16	<i>N. incompta</i> ; <i>N. pachyderma</i>	10/08/2023	10/08/2023	62.75	-37.51	20	10	34.9	2112	2305	8.09
CE23011_17	<i>N. pachyderma</i>	11/08/2023	11/08/2023	60.18	-39.13	50	6	34.91	2168	2299	8.09
CE23011_18	<i>N. pachyderma</i>	12/08/2023	13/08/2023	58.25	-45.64	45	7.5	34.66	2129	2185	7.89
CE23011_19	<i>N. pachyderma</i>	13/08/2023	14/08/2023	57.55	-48.52	35	6	34.7	2134	2296	8.11
CE23011_20	<i>N. incompta</i>	16/08/2023	17/08/2023	56.36	-27.89	10	14	35.04	2080	2311	8.09
HH24-PN-856	<i>N. pachyderma</i>	06/06/2024	06/06/2024	72.13	5.1	50	7.5	35.1	NA	NA	NA
HH24-PN-866	<i>T. quinqueloba</i>	07/06/2024	07/06/2024	71.21	11.5	50	8	35	NA	NA	NA



130 **Figure 1** Image showing the station locations for cruise CE23011 on the RV Celtic Explorer (2023). Stations S856 and S866 are the sampling sites for ARCLIM-24-1 cruise on the RV Helmer Hansen (2024). Map created using ODV (Schlitzer, 2022). Site symbol colour represents the ocean temperature at the tow depth of the sample site.

135 **2.2 Carbonate Chemistry**

Total alkalinity of seawater samples was determined onboard cruise CE23011 using an Apollo SciTech AS-ALK3 Total Alkalinity Titrator. This instrument operates on the principle of Gran titration, whereby approximately 0.1 M hydrochloric acid is incrementally added to 20 mL aliquots of seawater maintained at 20 °C. The resulting titration curve is used to construct a Gran function from which total alkalinity is calculated. The pH measurements 140 were conducted using an Orion 8302BNUMD Ross Ultra pH/ATC Triode probe, which was calibrated daily using Thermo Scientific buffer solutions at pH 4.01, 7.00, and 10.01. The concentration of the titrant (HCl) was standardised by titrating Certified Reference Material (CRM) Batch 208 for Oceanic CO<sub>2</sub> analysis, prepared by Dr. Andrew Dickson (Scripps Institution of Oceanography), a minimum of three times. Calibration was repeated until the relative standard deviation (RSD) of the calculated HCl concentration from at least two titrations was 145 below 0.01%. CRM Batch 208 was also used as a quality control standard, analysed approximately every fifth sample. When treated as a sample, Batch 208 yielded a standard deviation of 7.69 µmol/kg and an RSD of 0.35%. Replicate analyses were performed on every second sample, with an average difference of 8.43 µmol/kg and a relative average difference of 0.37%. Following titration, alkalinity values were converted from µmol/L to µmol/kg using the equation of state and subsequently corrected for instrumental drift using Batch 208.

150 DIC samples of seawater were collected in 500ml glass bottles and poisoned on board with 0.2ml mercuric chloride. DIC concentrations were measured with an LI-5350A DIC analyser coupled with an LI-850 infrared gas analyser. Briefly, 1.5 mL aliquots of seawater were acidified to convert all DIC to CO<sub>2</sub> gas, which was then



quantified by the gas analyser. Calibration of the DIC analyser was performed at the beginning and end of each analytical batch (comprising eight sample triplicates) using Batch 208 in triplicate volumes of 1.2 mL, 1.5 mL, 155 and 1.8 mL. Additional triplicate analyses of Batch 208 were conducted after each batch of eight sample triplicates to monitor instrument performance. Standard deviation of averages for Batch 208 triplicates was 1.35  $\mu\text{mol/kg}$  across all sample runs. Carbonate system parameters, including  $\Delta[\text{CO}_3]$ , were calculated from measured alkalinity and DIC using CO2sys version 25b06 (Lewis and Wallace, 1998). We used the equilibrium constants of Lueker et al. (2000), the  $\text{KSO}_4$  constant from Dickson, total boron from Uppström (1974), the KF from Dickson and Riley 160 (1979), and default values for  $\text{PO}_4^{3-}$  and  $\text{SiO}_2$  of 0 mol/kg.

### 2.3 Oxygen measurements

During CE23011, we performed single-specimen respiration measurements on board the RV Celtic Explorer within 24 hours of collection, using the same (filtered) seawater and temperature as foraminifera were collected 165 in. Given the large latitudinal gradient of the survey (e.g., 55 - 74°N), this allowed us to perform measurements over a large gradient for most ECVs analysed here. The following year, we collected foraminifera from a single station. We incubated them at different temperatures in the laboratory at UiT before performing respiration measurements in a temperature-controlled laboratory setting. This dual approach allowed us to evaluate the importance of food, rest and setting (ship vs lab) for the reproducibility of the results.

170 Measurements on single foraminifera were performed using the NanoRespiration system developed by Unisense™. It includes the Unisense MicroProfiling System coupled with a micro-rosette of seven fused glass capillaries ( $\varnothing = 0.68$  mm, length =  $3\pm0.2$  mm), a rosette holder and a metal frame which allows exact positioning and movement of the microsensor tip into the glass capillary (see Fig. 2 for set-up diagram). Oxygen profiles were measured using Clark-type microsensors of 50  $\mu\text{m}$  tip diameter with guard cathodes (Revbech, 1989), a fx-6 175 UniAMP multi-channel amplifier, and SensorTrace PRO v1.9 software from Unisense™. Each sensor was calibrated prior to each experiment using a 0% oxygen solution using either the premade ascorbate solution prepared by Unisense™ or dissolving Sodium Sulphite PryoScience™ capsules in 50 ml of distilled water and a 100% oxygenated seawater solution using filtered seawater and an aquarium pump.



180

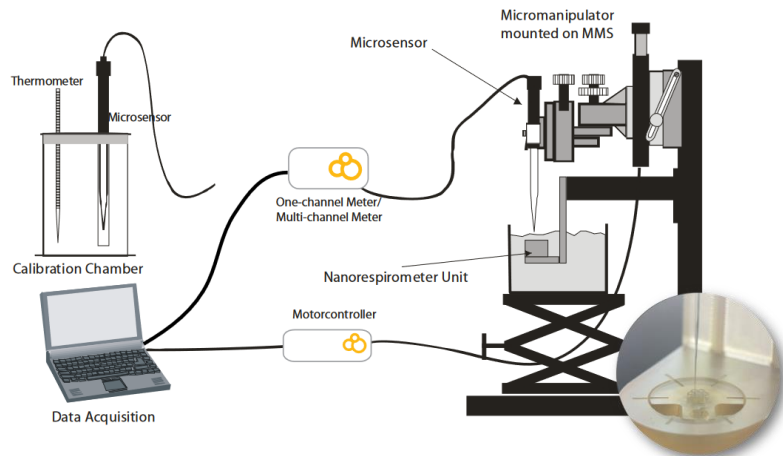


**Figure 2** Diagram adapted from Unisense (2025) showing the nano respiration set-up used to measure oxygen gradients on single foraminifera. The image on the bottom right shows a close-up of the Nanorespirometer Unit (e.g., rosette) and microsensor entering one of the glass capillaries.

185 Prior to analysis each glass capillary of the sample rosette was flushed with DI water and placed into an ultrasonic bath for 30 seconds. Once cleaned and DI water removed, the rosette was placed into a Petri dish filled with filtered seawater set at the precise temperature of incubation for each experiment. All glass capillaries were flushed with filtered seawater carefully removing any remaining bubbles in each capillary. Then, one living foraminifera (colourful, pseudopodia present) was placed per capillary, keeping one well empty as a control. The room temperature was maintained within 5 °C of the experiment temperature to avoid large fluctuations for the foraminifera during transfer from the incubator into the rosette. Once the transfer was complete, the loaded sample rosette was placed into the rosette holder and submerged in a jacketed beaker filled with filtered seawater at the exact temperature chosen for the experiment. Temperature was maintained to within 0.1°C using a Julabo circulator, circulating antifreeze into the jacket of the beaker. Foraminifera in the submerged rosette were 190 acclimated for 45-60 minutes. Seawater in the beaker was constantly agitated with air using an aquarium pump to maintain fully oxygenated seawater above the capillaries. Once acclimated the position of the sensor was calibrated using a micromanipulator, a PC-controlled motor unit (Woelfel et al., 2009) and a mounted dissecting microscope to ensure the sensor enters each capillary opening. Oxygen profiles were set to begin 400 µm above and end at 2000 µm inside each capillary, with step sizes of 200 µm. Measurements at each depth were performed 195 after allowing the sensor to equilibrate for 5 seconds, and each profile was repeated three times. The oxygen gradient in each capillary was measured using the average slope between 800 µm and 2000 µm inside the capillary for each triplicate measurement to determine individual respiration rate (IRR) measurements (Macuite et al., 2023) using Fick's first law of diffusion  $J = -D \times dC/dx$  where D is the oxygen diffusion coefficient at a given temperature (Broecker and Peng 1974), and  $dC/dZ$  is the measured oxygen gradient inside the capillary tube.

200 To account for background respiration, one capillary in each rosette was maintained as a blank, containing only seawater without any foraminifera. Respiration rates from these blanks were measured in triplicate, and the average value was subtracted from the respiration rates of the experimental chambers to yield a blank-corrected average respiration rate. Blank respiration values averaged at  $14.83 \pm 11.50 \text{ pmol h}^{-1} \text{ ind}^{-1}$ . Additional tests were



conducted using dead foraminifera specimens that had been previously dehydrated to assess background  
210 respiration in the absence of metabolic activity. Five dead specimens were tested, yielding an average respiration rate of  $17.00 \pm 5.83 \text{ pmol h}^{-1} \text{ ind}^{-1}$ , which is indistinguishable from the average procedural blank.

#### 2.4. Maximum diameter and cell volume reconstructions

Determining biovolumes using X-ray microcomputed tomography (Micro-CT) scanning for all individuals included in this study ( $n = 166$ ) was not feasible. We therefore opted to establish a robust empirical relationship  
215 between maximum diameter and cube root cavity volume for *T. quinqueloba*, *N. pachyderma*, and *N. incompta*, as previously suggested by Burke et al. (2020). Since the three species investigated exhibit similar low trochospiral coiling morphologies (Darling et al., 2006; El Bani Aluna et al., 2018; Pearson and Kucera, 2018), they are suited for this joint methodology and analysis. For micro-CT analysis tests were glued to a Kapton tube using a mix of tragacanth gum and **MQ** water, following a modified protocol from Coletti et al. (2018), Iwasaki et al. (2015),  
220 Siccha et al. (2023) and Fabbri et al. (2025). The Kapton tube was placed on a sample holder and scanned with the ZEISS Xradia 620 Versa, at the University of Galway.

The sample holder was placed between the X-ray source with a source-to-detector distance of 58 mm (Source-Rotation Axis distance: ~20mm; Detector-Rotation Axis distance 38 mm), providing a voxel resolution of 240 nm per pixel using the 20X objective magnification in binning 1 mode. The instrument was operated at 120 kV and  
225 17.5W, employing no energy filter to optimise transmission and the contrast-to-noise ratio. A total of 1601 radiographs were acquired over a 360° sample rotation range with an exposure time of 10 seconds per radiograph. The raw transmission images (.txrm) were reconstructed for each specimen using a commercial image reconstruction software package (ZEISS XMReconstructor) (ZEISS, 2024), which employs a filtered back-projection algorithm to generate the final reconstructed and corrected three-dimensional file. The final  
230 reconstructed files (.txm) were then exported as a stack of .tif image files for further study.

In addition, each foraminifer was imaged immediately after oxygen profiling using a Moticam X5 Plus (Motic Instruments Inc., [2024]) Wi-Fi camera mounted on a Zeiss Stemi 395 and the Motic Images Plus 3.1 ML software. After calibration, this software was used to measure the maximum diameter of the foraminifera in  $\mu\text{m}$ , completed under 64x magnification. The maximum diameter refers to the longest straight line that passes through the widest  
235 part of the foraminifera, typically measured through the final chamber (Fig. 4).

#### 2.5. Biometry

The exported micro-CT image stacks were segmented using the software *Amira 3D Pro* (Stalling et al., 2005). Manual thresholding was applied to isolate the tests and background, and the paintbrush tool was used to remove  
240 infilling or extraneous particles, such as cytoplasm. The segmented tests were rendered as volumes using the watershed algorithm. The maximum diameter was measured for all specimens using the measurement tool on the 3D volume rendering of the test in the same orientation as the optical microscope. The internal voids of all chambers were then isolated and rendered as a separate volume using the “Ambient Occlusion” function in *Amira 3D Pro*, which filled the negative volume virtually (Baum and Titschack, 2016; Titschack et al., 2018). The  
245 internal volume of the combined chambers and of the pores within the test wall (Fig. 4) was then measured using



the label analysis function in Amira (Kiss et al., 2023).

Respiration rates were analysed in two ways. First, we used cell volume to size-normalise respiration rates and evaluate the response of the specimens to changes in temperature and other essential climate variables. A common way to estimate the influence of temperature on a physiological rate is the use of the  $Q_{10}$  value, which quantifies the rate increase for a 10 °C increase.  $Q_{10}$  was calculated following Eq. (1) (adapted from Schmidt-Nielsen, 1997):

$$\log_{10} Q_{10} = (\log_{10} R_2 - \log_{10} R_1) \cdot \frac{10}{(T_2 - T_1)} \quad (\text{Eq.1})$$

Where  $R_2$  is the respiration rate at the higher temperature,  $R_1$  is the respiration rate at the lower temperature,  $T_1$  is the lower temperature, and  $T_2$  is the higher temperature. It is essential to recognise that, although the use of a  $Q_{10}$  is a convenient measure, it varies as a function of the temperature range being considered (Lombard et al., 2009). For example, when calculating the  $Q_{10}$  value for *N. pachyderma*, we excluded the lab-based experiment at 13 °C since it lies outside of this species' typical habitat range.

Secondly, we normalised respiration rates to 5°C, 15°C and 24°C to evaluate the influence of cell volume on respiration rates. 24°C was chosen to facilitate comparative analysis with previous work, particularly that of Lombard et al. (2009), thereby enabling meaningful contextual interpretation of the current dataset. 15°C represented a thermal midpoint across all experiments, minimising physiological deviation and ensuring that species were assessed under temperatures approximating their average environmental exposure. 5°C served as the low-temperature condition, selected for its relevance for *N. pachyderma*, the focal species of this investigation. Using a  $Q_{10}$  value of 3.18 from Lombard et al. (2009), and  $Q_{10}$  values derived for *N. pachyderma*, *N. incompta* and *T. quinqueloba* in this study (see Table 4) following Eq. (2):

$$R_x = R_t \cdot Q_{10}^{\frac{24-t}{10}} \quad (\text{Eq.2})$$

Where  $R_x$  is the respiration rate at X °C,  $R_t$  is the respiration rate at the measured temperature, and t is the measured temperature.

### 3. Results

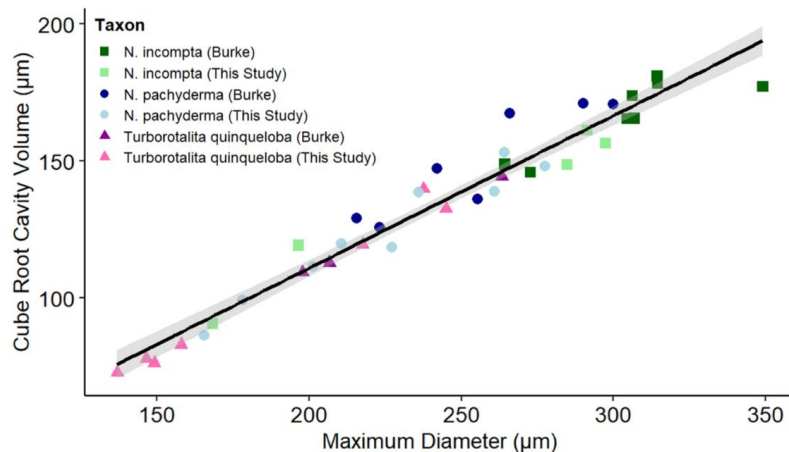
#### 270 3.1. Cell volume reconstructions

Cavity volume and maximum diameter using micro-CT scans were assessed for a subset of 39 specimens (23.5%). These include 19 new specimens from this study (e.g., *N. pachyderma* (n=7), *N. incompta* (n=5), and *T. quinqueloba* (n=7) and the reanalysis of 20 .tiff stacks of scanned *N. pachyderma* (n=9), *N. incompta* (n=8) and *T. quinqueloba* (n=3) previously published in Burke et al. (2020). An independent paired student t-test comparing the maximum diameters reported in Burke et al. (2020) and the measurements of the same scans using Amira in the current study had a p-value of <0.01, (95% Confidence Interval (C.I.) [1.65-7.4 4µm]) meaning there is a 0.61% to 2.75% difference between measurements reported in Burke et al. (2020) and reported here for the same foraminifera.



280 **Table 2** Summary of maximum diameter and cube root volume measurements of the 39 specimens that were scanned for volume reconstructions.

	<i>N. pachyderma</i> [n=16]	<i>N. incompta</i> [n=13]	<i>T. quinqueloba</i> [n=10]
<b>Mean max Ø [µm]</b>	244.3	284.2	195.8
<b>Range Ø [µm]</b>	165.48 to 315.5	168.36 to 349.08	136.91 to 263.33
<b>Mean biovolume <math>\sqrt[3]{V}</math> [µm]</b>	136.3	160.14	106.8
<b>Biovolume range <math>\sqrt[3]{V}</math> [µm]</b>	86.33 to 171.11	119.19 to 180.99	72.76 to 144.25
$\sqrt[3]{V}$ cavity volume = a(max Ø) + b	a = 0.61; b = -10.31	a = 0.50; b = +13.19	a = 0.60; b = -10.51
	$r^2 = 0.90$ ; p < 0.01	$r^2 = 0.93$ ; p < 0.01	$r^2 = 0.99$ ; p < 0.01



285 **Figure 3** Combined max Ø (µm) vs  $\sqrt[3]{V}$  cavity volume (µm) for *N. pachyderma*, *N. incompta* and *T. quinqueloba* showing trendline, slope and  $R^2$  value. The source data for this figure is available in Table S2

285

The relationship between the  $\text{maxØ}$  (µm) and  $\sqrt[3]{V}$  cavity volume for all 39 specimens analysed here (Fig. 3) follows Eq. (3):

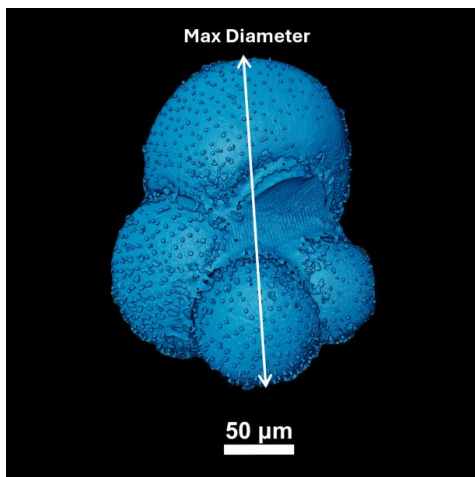
$$\sqrt[3]{V} \text{ cavity volume} = (0.56 \pm 0.02) \text{maxØ} + (-0.38 \pm 5.47) \quad (\text{Eq.3})$$

290 n = 39,  $r^2 = 0.95$ , p < 0.01. For species-specific equations, please see Table 2. Volume reconstructions performed in this study are significantly smaller than previous estimates that are based on the assumption that the cavity volume corresponds to 75% of the closest geometric shape (e.g., sphere for species analysed) that can be fitted around the maximum diameter of the foraminifera (e.g., Hannah et al., 1994; Geslin et al., 2011; Cesbron et al., 2016; Macuite et al. 2023). A comparison of both techniques shows that using 75% of a sphere to estimate cavity volume overestimates actual biovolume by  $47 \pm 7.37\%$ . Specifically, for each of the species analysed, the 295 relationship between the volume of a sphere based on the max Ø (µm) and micro-CT-based cavity volume reconstructions was  $35.36 \pm 4.57\%$  for *N. pachyderma*,  $33.21 \pm 6.09\%$  for *N. incompta* and  $37.69 \pm 5.67\%$  for *T. quinqueloba*. We also note that the protocol for analysing cavity volumes used in this study led to significantly smaller cavity volumes (28% difference, paired t-test p>0.01) when compared to Burke et al. (2020).

The main difference between methods is that we used the ambient occlusion function in Amira (Titschack et al.,



300 2018), which allows the segmentation of the shell and measurements of the internal volume of the tests, excluding the shell, while in Burke et al. (2020) external meshes were imported into MeshLab software, where they were resurfaced and replaced with watertight “wrap” mesh, which closes all apertures and pores, allowing the interment of the cavity volume of the entire test by subtracting the  $\text{CaCO}_3$  volume from the wrap volume. This method appears to overestimate cavity volumes, since the reported cavity volumes exceed the volume of a sphere fitted to  
305 the maximum diameter of each test by a mean of  $115 \pm 27\%$  for *N. incompta*,  $137 \pm 20\%$  for *N. pachyderma* and  $179 \pm 6\%$  for *T. quinqueloba*.



310 **Figure 4:** Example of volume rendering of a specimen of *N. pachyderma* selected for 3D volume analysis in Amira 3D Pro. This figure shows the internal voids of the chambers, porosity, and the white line indicates the maximum diameter (Max Diameter) for this specimen. Scale bar 50  $\mu\text{m}$ .

### 3.2. Respiration Rates

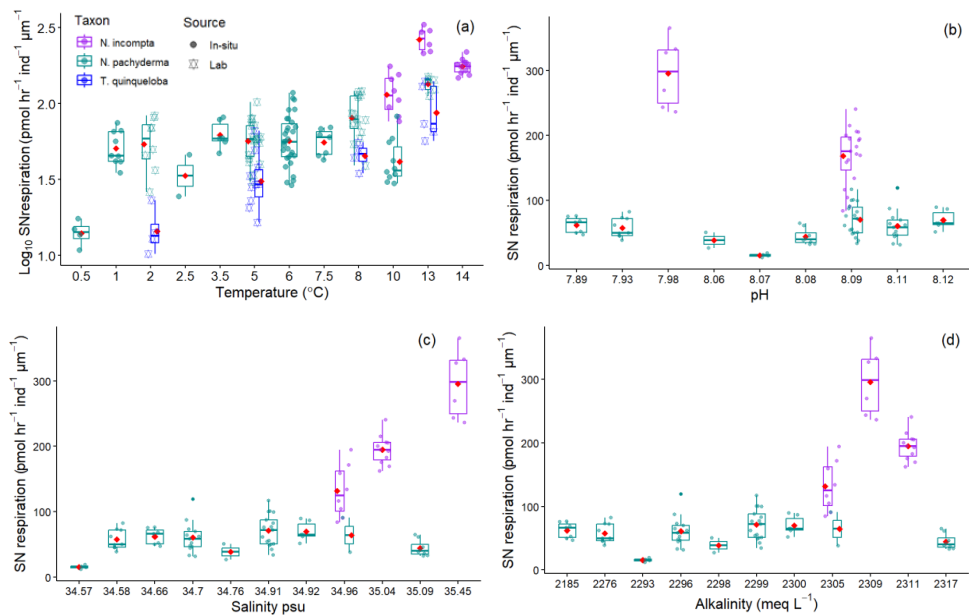
Here we use the multispecies relationship between  $\sqrt[3]{\text{cavity volume}} (\mu\text{m})$  and  $\text{max } \varnothing (\mu\text{m})$  defined in section 3.1.  
315 to size-normalise the respiration rates. For the ship-based CE23011 cruise dataset from 2023, we recorded mean size-normalised respiration rates of  $59.22 \text{ pmol hr}^{-1} \text{ ind}^{-1}$  (95% C.I. [53.32 - 65.13]) for *N. pachyderma* over a temperature gradient of  $9.5^\circ\text{C}$  measured between  $0.5 - 10^\circ\text{C}$ . For *N. incompta* we record higher mean size-normalised respiration rates of  $198.99 \text{ pmol hr}^{-1} \text{ ind}^{-1}$  with a larger variability (95% C.I. [169.48-228.50]) analysed over a smaller temperature gradient of  $4^\circ\text{C}$  measured between  $10^\circ\text{C}$  and  $14^\circ\text{C}$ . For the laboratory-based dataset  
320 (Tromsø 2024), the mean size-normalised respiration rates for *N pachyderma* were comparable to the ship-based data (e.g.,  $62.71 \text{ pmol hr}^{-1} \text{ ind}^{-1}$  (95% CI: [57.45, 67.97])). Mean size-normalised respiration rates for *T. quinqueloba*, are also low at  $45.75 \text{ pmol hr}^{-1} \text{ ind}^{-1}$  with low variability (95% CI: [31.99, 59.50]) over a temperature gradient of  $11^\circ\text{C}$  measured between  $2-13^\circ\text{C}$  for both species. While Hemleben (1989) and Stangeew et al., (2001) noted the presence of symbionts in *T. quinqueloba*, their presence remains elusive in other studies (e.g., Takagi et  
325 al., 2019; Hoogakker et al. (2022); Kanbur, 2025), and none of the specimens analysed in this study bore symbionts. Thus, calculated respiration rates were not for adjusted photosynthesis as in Lombard et al. (2009) for

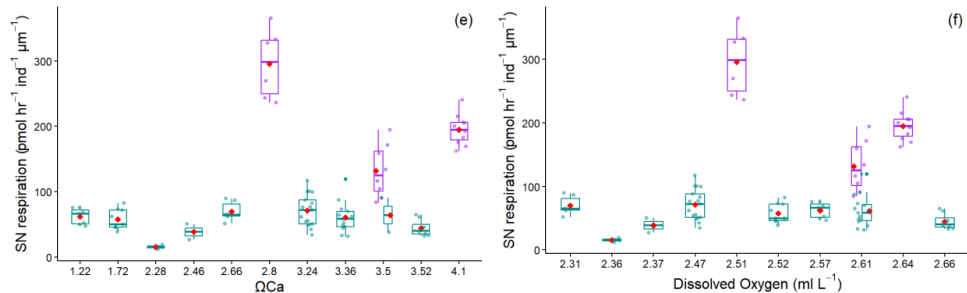


*O. universa*, *G. ruber* and *G. siphonifera*.

The sensitivity of size-normalised respiration rates and temperature for tropical and subtropical planktonic foraminifera is best described by an exponential or Arrhenius relationship, rather than a simple linear one (Lombard et al., 2009). We therefore plot the log<sub>10</sub> size-normalised respiration rates (pmol hr<sup>-1</sup> ind<sup>-1</sup> μm<sup>-1</sup>) against temperature for our analysis. The log<sub>10</sub> size-normalised respiration rates (pmol hr<sup>-1</sup> ind<sup>-1</sup> μm<sup>-1</sup>) against temperature are shown in Fig. 5a for all species. For all other essential climate variables such as, pH, salinity, alkalinity, Ω<sub>Ca</sub>, dissolved oxygen (Fig. 5), SiO<sub>2</sub> (μM), Dissolved Inorganic Carbon, PO<sub>4</sub><sup>3-</sup> (μM), and Total Organic Nitrogen (μM), size-normalised respiration rates are shown in Fig 5 b-f and Fig. 6. In Table 3 we report correlation statistics for each variable and show that there is no significant correlation between respiration rates of *N. pachyderma* and any of the ECVs measured here. For *N. incompta* we have a more limited dataset measured over a narrower range in environmental gradients and find significant correlations notable for temperature, SiO<sub>2</sub>, salinity, fluorescence, dissolved O<sub>2</sub>, pH and Ω<sub>Ca</sub> (Table 3). A detailed correlation matrix, which explores these relationships further, is available in Table S1.

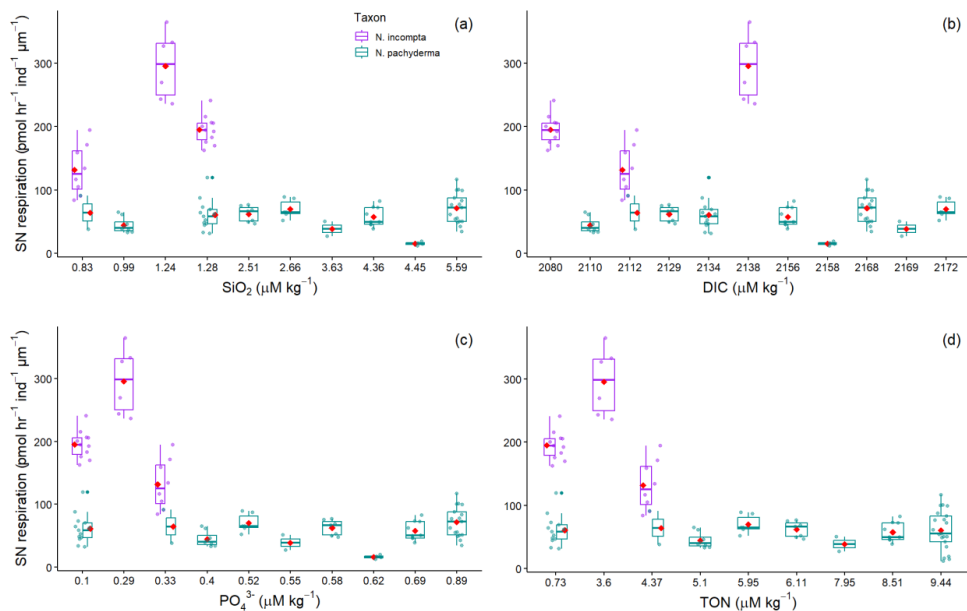
Correlation statistics, between log<sub>10</sub> size-normalised respiration and temperature and Q<sub>10</sub> values are reported in Table 4 for all species. We find that temperature accounts for a greater proportion of the variance in respiration for *N. incompta* ( $r^2 = 0.45$ ) and *T. quinqueloba* ( $r^2 = 0.71$ ) than for *N. pachyderma* ( $r^2 = 0.05$ ). The sensitivity to temperature is explained by the Q<sub>10</sub> values determined for each species. *N. pachyderma* exhibits a low Q<sub>10</sub> of 1.41 between 0.5°C and 10 °C. In contrast, *N. incompta* and *T. quinqueloba* demonstrate a much higher Q<sub>10</sub> of 3.58 and 4.53 over 10-14°C and 2-13°C, respectively.





350 **Figure 5:** Box and whisker plots of the effect of essential climate variables on Size Normalised Respiration based on biovolume ( $\text{pmol hr}^{-1} \text{ind}^{-1}$ ) in *N. pachyderma*, *N. incompta* and *T. quinqueloba* (a) Temperature  $^{\circ}\text{C}$  and (b) pH; (c) Salinity (psu) and (d) Alkalinity ( $\text{meq L}^{-1}$ ); (e)  $\Omega\text{Ca}$  and (f) Dissolved Oxygen ( $\text{ml L}^{-1}$ ). Boxes extend from the data's lower to upper quartile values, with a line at the median. Whiskers indicate 1.5 times the interquartile distance. Red dots mark the mean. Log<sub>10</sub> Size normalised respiration and laboratory data are only available for (a). The source data for this figure is available in Tables S3 and S4.

355



360

**Figure 6:** Box and whisker plots of the effect of nutrients on Size Normalised Respiration based on Biovolume ( $\text{pmol hr}^{-1} \text{ind}^{-1}$ ) in *N. pachyderma* and *N. incompta*. (a)  $\text{SiO}_2$  ( $\mu\text{M kg}^{-1}$ ) and (b) Dissolved Inorganic Carbon ( $\mu\text{M kg}^{-1}$ ); (c)  $\text{PO}_4^{3-}$  ( $\mu\text{M kg}^{-1}$ ) and TON ( $\mu\text{M kg}^{-1}$ ). Boxes extend from the lower to upper quartile values of the data, with a line at the median. Whiskers indicate 1.5 times the inter-quartile distance. The red dots mark the means. The source data for this figure is available in Table S3 and S4

365

**Table 3:** Quantification of the correlations between size-normalised respiration and essential climate variables and nutrients in *N. pachyderma* and *N. incompta*. Blue shading denotes significant correlations ( $p \leq 0.01$ ), while orange shading indicates lower levels of statistical significance.

<i>N. pachyderma</i>		<i>N. incompta</i>	
<i>n</i> =72		<i>n</i> =28	
$r^2$	p-value	$r^2$	p-value



<b>TON</b>	0.001	$p=0.85$	0.010	$p=0.64$
<b>PO<sub>4</sub></b>	0.028	$p=0.18$	0.005	$p=0.74$
<b>SiO<sub>2</sub></b>	0.026	$p=0.19$	0.374	$p=0.001$
<b>Salinity</b>	0.022	$p=0.23$	0.694	$p<0.001$
<b>Turbidity</b>	0.001	$p=0.85$	0.003	$p=0.814$
<b>Fluorescence</b>	0.002	$p=0.70$	0.602	$p<0.001$
<b>DIC</b>	0.040	$p=0.1$	0.160	$p=0.047$
<b>Dissolved O<sub>2</sub></b>	0.001	$p=0.83$	0.428	$P<0.001$
<b>Alkalinity</b>	0.003	$p=0.66$	0.206	$p=0.02$
<b>pH</b>	0.002	$p=0.72$	0.602	$p<0.001$
<b>ΩCa</b>	0.007	$p=0.5$	0.228	$p=0.008$

**Table 4:** Quantification of the correlations and  $Q_{10}$  between  $\log_{10}$  size-normalised respiration and temperature in *N. pachyderma*, *N. incompta* and *T. quinqueloba* for in-situ (2023) and laboratory (2024) measured respiration.

Species	Source	n	Range (°C)	$Q_{10}$	SD	$r^2$	p-value
<i>N. pachyderma</i>	In-situ	68	0.5-10	1.41	0.203	0.05	$p = 0.08$
<i>N. incompta</i>	In-situ	25	10-14	3.58	0.162	0.45	$p < 0.01$
<i>T. quinqueloba</i>	Lab data	23	2-13	4.53	0.29	0.71	$p < 0.01$

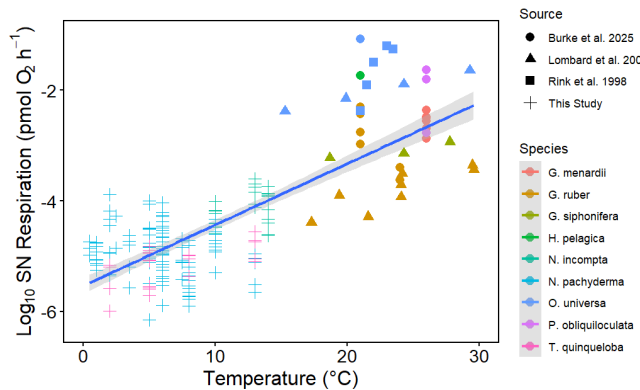
370 **3.3. Comparison to previously published respiration rates on planktonic foraminifera**

To quantify the effect of temperature on size-normalised respiration rates, we combined our dataset with previous studies carried out by Lombard et al. (2009) on *Orbulina universa*, *Globigerinoides ruber* and *Globigerinella siphonifera*, by Rink et al. (1998) on *O. universa* and Burke et al. (2025) on *Globorotalia menardii*, *Pulleniatina obliquiloculata*, *Hastigerina pelagica*, *O. universa* and *G. ruber*. (Fig. 7). Cell volumes for *N. pachyderma*, *N. incompta* and *T. quinqueloba* were computed using the relationship between cavity volume and maximum diameter (Fig. 3) derived in this study. Results show that the respiration rates of all planktonic foraminifera included here follow Eq. (4):

$$\log_{10} R_{\text{biovolume}} = 0.11t - 5.54 \quad (\text{Eq.4})$$

Where  $R_{\text{biovolume}}$  is the respiration rate normalised by biovolume, and  $t$  is the temperature at which the respiration rate was measured ( $r^2 = 0.62$ ,  $n = 201$  and  $p < 0.001$ ). We found that when normalised to 5 °C, 15 °C and 24 °C (Fig. 8), respiration rates scale positively with biovolume across all datasets. The relationships are best described by linear regression following:

$$Rx = m \cdot BV + c \quad \text{Eq. (5):}$$

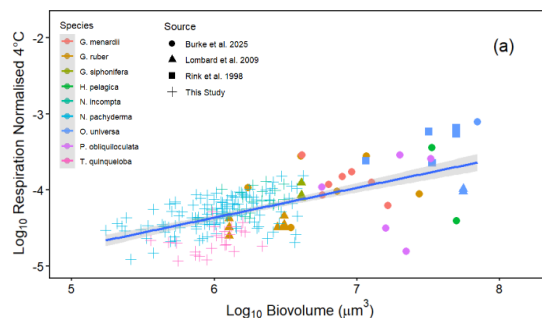


385 **Figure 7:** The effect of temperature (°C) on  $\log_{10}$  size-normalised respiration rate ( $\text{pmol O}_2 \text{ hr}^{-1} \text{ ind}^{-1} \mu\text{m}^{-1}$ ) in this study and previously published data (Rink et al., 1998; Lombard et al., 2009 and Burke et al., 2025). The grey shaded regions represent the 95% confidence bounds of the regression model. The source data for this figure is available in Table S5

The relationships described by Eq. (5) across different temperatures are:

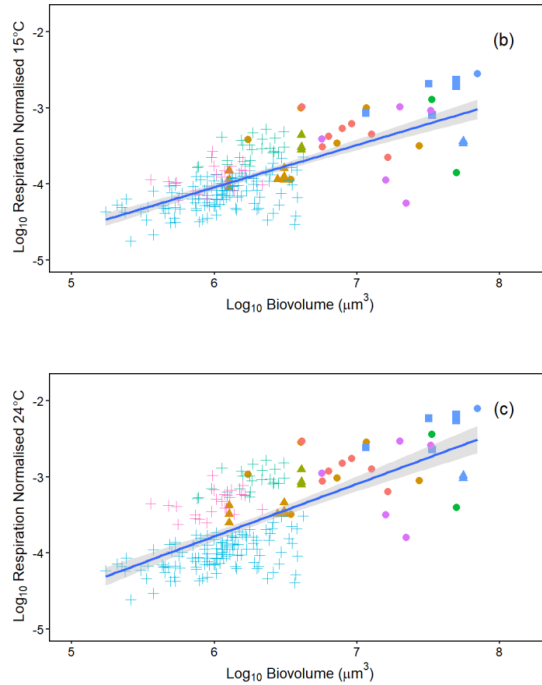
390 (a)  $R_4 = 0.39 \pm 0.03BV - 6.72 \pm 0.21(r^2 = 0.4, n = 201, p < 0.01)$   
 (b)  $R_{15} = 0.56 \pm 0.04BV - 7.38 \pm 0.24(r^2 = 0.51, n = 201, p < 0.01)$   
 (c)  $R_{24} = 0.69 \pm 0.05BV - 7.93 \pm 0.34(r^2 = 0.48, n = 201, p < 0.01)$

Where  $R_x = \log_{10}$  respiration rate normalized to  $x^\circ\text{C}$  and  $BV = \log_{10}$  Biovolume ( $\mu\text{m}^3$ ). The steepest slope occurs when normalizing to  $24^\circ\text{C}$  ( $R_{24} = 0.69 \pm 0.05$ ), followed by  $15^\circ\text{C}$  ( $R_{15} = 0.56 \pm 0.04$ ), and  $4^\circ\text{C}$  ( $R_4 = 0.39 \pm 0.03$ ).  
 395  $R^2$  values range between 0.40 and 0.51, indicating that while biovolume is a significant predictor of respiration, other biological or environmental factors likely contribute to the observed variability. Nevertheless, the consistent significance ( $p < 0.01$ ) across all regressions underscores the robustness of the biovolume-respiration relationship.





400



405

**Figure 8** Scaling of individual planktonic respiration rates as a function of estimated biovolume with respiration normalised either using species-specific  $Q_{10}$ s established in this study or a uniform  $Q_{10}$  of 3.18 from Lombard et al., 2009. Data includes previously published sources (Rink et al., 1998; Lombard et al., 2009 and Burke et al., 2025). Panels show normalisation to (a) 4 °C, (b) 15 °C and (c) 24 °C. Grey shaded regions represent the 95% confidence intervals of the regression models. The source data for this figure is available in Table S8

## 4. Discussion

### 4.1 Respiration Rates and Environmental Stability

One of the most striking findings of this study is the metabolic stability of *N. pachyderma* across a wide range of ECVs and nutrients. Respiration rates in *N. pachyderma* are stable across pH (7.89–8.12), salinity (34.57–35.09 psu), dissolved oxygen (2.31–2.66 ml/L), alkalinity (2185–2317 meq/L), and  $\Omega_{\text{Ca}}$  (1.22–3.52) as well as nutrients (Fig. 6). This physiological resilience suggests that the polar genotype of *N. pachyderma* (Type I in Darling et al., 2004) evolved to adapt to the extreme and variable environment of the Arctic Ocean. Only when exposed to temperatures outside of its habitat range in the laboratory (e.g., 13°C), we recorded a small but significant increase in respiration rate.

The low thermal sensitivity of *N. pachyderma*, is reflected in a  $Q_{10}$  value of 1.41 (Table 4) across the 0.5 °C to 10 °C range (based on ship-based data) and suggests a successful physiological adaptation to cold environments. Low  $Q_{10}$  values have been interpreted as characteristic of the optimal temperature range of a species in its natural habitat (Wieser, 1973). This suggests that *N. pachyderma* (Type I) functions at its metabolic optimum in present-day Arctic conditions. Notably, respiration rates do not decline at the low temperatures measured, unlike in other

420



species, which often exhibit constrained metabolic activity under extreme cold conditions.

Molecular evidence presented by Darling et al., (2004, 2007) suggests that the *N. pachyderma* population presently living at high northern latitudes became isolated during the onset of Northern Hemisphere Glaciations, between 1.8 and 1.5 million years ago, a period marked by the expansion of the polar ice sheets and the 425 establishment of persistently cold oceanic conditions. Furthermore, Kucera and Kennett (2002) proposed that the species-specific cold-water affinity of *N. pachyderma* may have evolved in response to the onset of the 100,000-year glacial-interglacial climate cycles during the Middle Pleistocene. Furthermore, an increase in *N. pachyderma* shell sizes over the last 1.1 million years may represent an adaptive response to cold environments of the Quaternary (Huber et al. 2000). The current polar affinity of *N. pachyderma* may thus represent an evolutionary 430 legacy of this climatic transition.

Likewise, spinose planktonic foraminifera such as *T. quinqueloba* exhibit distinct evolutionary and physiological traits that reflect their adaptation to surface ocean environments. Their spines enhance prey capture and buoyancy and often support photosymbiotic relationships with algae (though no symbionts were seen in this study), enabling 435 survival in oligotrophic waters (Anderson & Bé, 1976; Hemleben et al., 1989). In this study, *T. quinqueloba* displayed a high  $Q_{10}$  value of 4.54, indicating that this subpolar species exhibits a particularly strong temperature dependence, which is likely to impact its metabolism, potentially affecting its growth and overall survival (Mundim et al. 2020). This contrasts with the lower  $Q_{10}$  of 1.41 observed in the non-spinose, *N. pachyderma*, but is consistent with  $Q_{10}$  values around 3.18 derived for other spinose species such as *G. ruber*, *G. siphonifera*, and 440 *O. universa* (Lombard et al. 2009), suggesting divergent thermal strategies linked to morphology and trophic mode. The metabolic divergence observed here between spinose and non-spinose planktonic foraminifera likely contributes to the latitudinal partitioning of planktonic foraminiferal assemblages, with spinose taxa dominating tropical zones and non-spinose forms prevailing in subpolar and polar regions (Bé & Tolderlund, 1971, Ying et al., 2023). However, even within closely related species such as *N. incompta* and *N. pachyderma*, our observations 445 suggest that the metabolic response to environmental conditions varies across foraminiferal taxa (Lombard et al. 2009).

#### 4.2 Volume Scaling and Metabolic Allometry

While a positive log-log relationship between biomass, weight or volume and respiration is usually observed in micro/meiofauna (e.g. Fenchel and Finlay, 1983; Gerlach et al. 1985; Moens et al., 1999; Moodley et al., 2008), mixed results have been reported for this relationship in foraminifera. Some studies have found a positive 450 correlation (Bradshaw et al. 1961; Geslin et al., 2011; Macuite et al. 2023), while others have not (Hannah et al., 1994; Nomaki et al., 2007). However, neither Hannah et al. (1994) nor Nomaki et al. (2007) use micro CT scanning to estimate biovolumes. Nomaki et al. (2007) used the relationship between test size and organic content (Altenbach, 1985), while Hannah et al. (1994) used 75% of the best-fitting geometric shape to estimate total internal test volume, a methodology with potential issues as suggested in section 3.1. above. Our results showed 455 a positive linear correlation between respiration and biovolume (Fig. 8) across the polar and subpolar populations of *N. pachyderma*, *N. incompta*, and *T. quinqueloba*, consistent with pelagic foraminiferal species exclusively growing in warmer subtropical and tropical oceans (Burke et al., 2025; Lombard et al., 2009 and Rink et al., 1998). This supports earlier findings that body size is a significant determinant of metabolic rate in foraminifera (Rink et



al., 1998; Geslin et al., 2011).

460 Furthermore, our analysis (Fig. 8) reveals a consistent and positive scaling relationship between biovolume and respiration rates across all temperature normalisations (5 °C, 15 °C, and 24 °C). This demonstrates that larger planktonic foraminifera exhibit higher metabolic rates, even when respiration is normalised to account for temperature effects using both species-specific and uniform  $Q_{10}$  values (Table 4). In panel (b) of Fig. 8, which shows respiration normalised to 15 °C, we observe a crossover point in size-normalised respiration rates for *N. incompta* and *N. pachyderma*. This intersection suggests a potential physiological tipping point below 15 °C, where the metabolic efficiency of *N. pachyderma* begins to exceed that of *N. incompta*. This aligns with observed shifts in assemblage dominance across temperature gradients, with *N. pachyderma* prevailing in colder polar waters and *N. incompta* in subpolar to temperate regions (Bé and Hutson, 1977; Al-Sabouini et al., 2007; Husum and Hald, 2012; Chaabane et al., 2024). This crossover may reflect species-specific thermal sensitivities and could 465 play a role in defining their biogeographic boundaries. It also highlights the value of using species-specific  $Q_{10}$  values to resolve fine-scale metabolic differences that may underlie broader ecological patterns.

470

Our results are broadly consistent with Kleiber's Law, which predicts sublinear scaling of metabolic rate with body size (Kleiber, 1932). We observed positive, sublinear relationships between respiration and biovolume across all temperature-normalised datasets, with slopes increasing from 0.39 at 5 °C to 0.69 at 24 °C. While Kleiber's 475 canonical  $\frac{3}{4}$  exponent is not fully met, the trend supports the principle that larger foraminifera have higher, but less-than-proportional, metabolic rates. Interestingly, DeLong et al. (2010) showed that metabolic scaling varies across evolutionary transitions—being super linear in prokaryotes, linear in protists, and sublinear in metazoans. Our findings place planktonic foraminifera, unicellular eukaryotes, closer to metazoan-like metabolic behaviour, possibly due to their structural complexity, calcification, or ecological specialisation. This suggests that metabolic 480 constraints in foraminifera may reflect both their unicellular nature and their functional convergence with more complex organisms.

#### 4.3 Proxy Reliability

A central concern for proxy-based climate reconstructions is the potential impact of physiological processes on shell geochemistry (Pérez-Huerta and Andrus, 2010). Variations in calcification and respiration rate in non-spinose 485 species can alter pH and carbonate chemistry in the foraminiferal microenvironment, potentially affecting Mg/Ca,  $\delta^{11}\text{B}$ ,  $\delta^{18}\text{O}$  and  $\delta^{13}\text{C}$  values in (Wolf-Gladrow et al., 1999; Zeebe and Sanyal, 2002). However, our data show that respiration in *N. pachyderma* remains stable across both temperature and pH gradients typically encountered in its natural range (Fig. 5). Respiration rates are also consistent and stable across a large range of other ECVs measured, suggesting that respiration is unlikely to introduce significant uncertainties into geochemical-based 490 palaeotemperature reconstructions for this species. These results also agree well with the recent  $\delta^{11}\text{B}$ -pH calibration for *N. pachyderma* that shows  $\delta^{11}\text{B}$  values for this species are consistently offset from seawater borate (de la Vega et al., 2025). Consequently, our findings alleviate concerns about physiological confounding due to 495 respiration. However, this may not be the case for *N. incompta* and *T. quinqueloba*. The elevated  $Q_{10}$  values for these two species may call for the development of species-specific calibration equations that consider the influence of respiration for accurate proxy application.

#### 4.4 Conclusions



By avoiding overestimation biases inherent in geometric models, micro-CT-derived biovolumes strengthen the foundation for future studies on respiration in foraminifera. These methodological improvements enhance the accuracy of single-specimen respiration rate assessments and facilitate more accurate interspecies comparisons.

500 Furthermore, our study demonstrates that there is no significant relationship between respiration and temperature or other ECVs (salinity, pH, dissolved oxygen, alkalinity, and  $\Omega_{\text{Ca}}$ ) or nutrients ( $\text{SiO}_2$ , DIC,  $\text{PO}_4^{3-}$ , and TON) in *N. pachyderma*, suggesting this polar species has a strong thermal resistance and is well adapted to its unique environment. On the other hand, *T. quinqueloba* and *N. incompta* exhibit a statistically significant relationship between respiration and temperature, demonstrating large physiological diversity among planktonic foraminifera 505 inhabiting overlapping climate zones. Additionally, we demonstrate a strong relationship between biovolume and respiration rate, underscoring the importance of size grading when using proxies. We conclude that for *N. pachyderma* respiration is unlikely to influence geochemical climate proxies.

#### **Data and materials availability**

510 All data needed to evaluate the conclusions in the paper are presented in the paper and/or the Supplementary Materials.

#### **Author contributions**

D.A. carried out respiration measurements at UiT and carried out micro-CT scanning at the University of Galway.  
515 In addition, she compiled and analysed all datasets and wrote the original draft of the manuscript. A.M. conceptualized the project, acquired funding, designed and carried out respiration experiments on board the Celtic Explorer (CE23011) as well as in the laboratory at UiT. In addition, she supervised D.A. in all data analysis and writing of the original draft. N.G. supported method development, experimental design, and respiration measurements during CE23011 and contributed to the final version of this manuscript. T.L.W. and E.D.V  
520 performed Alkalinity and DIC measurements on board CE23011 and at the Marine Institute and contributed to the final version of this manuscript. In addition, T.L.W. supported D.A. with micro-CT scanning and analysis of images using AMIRA. M.M.E. was the chief scientist on the ARCLIM-24-1 cruise on the RV Helmer Hansen, supported the collection of live foraminifera, provided culturing facilities, and contributed to the final version of this manuscript. A.W., F.S. and A.F. supported the collection of live foraminifera during both expeditions and 525 contributed to the final version of this manuscript. In addition, A.F. supported D.A. with micro-CT scanning and analysis of images using AMIRA. J.M. provided support in collection and culturing of live foraminifera during both expeditions and contributed to the final version of this manuscript. T.L.B. contributed to discussions on the initial conceptualization of the experimental design and method development of the nano-respiration system.

#### **530 Competing interests**

The contact author has declared that neither they nor their co-authors have any competing interests.



### Funding Sources

A.M. acknowledges funding by Research Ireland and the Geological Survey of Ireland under the SFI Frontiers  
535 for the Future Programme 21/FFP-P/10261 and Grant in Aid funding from the Marine Institute for research  
expedition CE23011 on the RV Celtic Explorer. N.G. acknowledges funding from the Deutsche  
Forschungsgesellschaft (DFG) under grant number GL 999/3-1. M.M.E, F.S and A.W. acknowledge funding  
from ARCLIM a Tromsø Research Foundation (TFS) starting grant project, with grant number: A31720.

### Acknowledgements

540 We gratefully acknowledge the support of the crew on the RV Celtic Explorer sailing under Master Anthony  
Hobin.

### 5. References:

Al-Sabouni, N., Kucera, M., and Schmidt, D. N.: Vertical niche separation control of diversity and size disparity  
545 in planktonic foraminifera, *Marine Micropaleontology*, 63, 75–90,  
<https://doi.org/10.1016/j.marmicro.2006.11.002>, 2007.

Altenbach, A. V.: Die biomasse der benthischen foraminiferen: auswertungen von "Meteor"-expeditionen im  
östlichen nordatlantik, PhD Thesis, Christian-Albrechts-Universität, 1985.

Anderson, O. R., Spindler, M., Bé, A. W. H., and Hemleben, Ch.: Trophic activity of planktonic foraminifera, *J.  
550 Mar. Biol. Ass.*, 59, 791–799, <https://doi.org/10.1017/S002531540004577X>, 1979.

Anglada-Ortiz, G., Rasmussen, T. L., Chierici, M., Fransson, A., Ziveri, P., Thomsen, E., Zamelczyk, K.,  
Meiland, J., Ezat, M. M., and Garcia-Orellana, J.: Changes in Planktic Foraminiferal Distribution, Productivity,  
and Preservation in the Barents Sea During the Last Three Millennia, *Paleoceanography and Paleoclimatology*,  
40, e2024PA004989, <https://doi.org/10.1029/2024PA004989>, 2025.

555 Baum, D. and Titschack, J.: Cavity and Pore Segmentation in 3D Images with Ambient Occlusion, *EuroVis '16:  
Proceedings of the Eurographics / IEEE VGTC Conference on Visualization: Short Papers*, 113-117,  
<https://dl.acm.org/doi/abs/10.5555/3058878.3058902>, 2016

Bé, A. W. and Hutson, W. H.: Ecology of planktonic foraminifera and biogeographic patterns of life and fossil  
assemblages in the Indian Ocean, *Micropaleontology*, 369–414, <https://doi.org/10.2307/1485406>, 1977.

560 Bé, A. W. and Tolderlund, D.S. 1971.: Distribution and ecology of living planktonic foraminifera in surface  
waters of the Atlantic and Indian Oceans, in: *The Micropalaeontology of the Oceans*, edits by: Funnel, B.M. and  
Riedel, W.R., Cambridge University Press, London, 105-149, 1971.

Bertlich, J., Gussone, N., Berndt, J., Arlinghaus, H. F., and Dieckmann, G. S.: Salinity effects on cultured  
*Neogloboquadrina pachyderma* (sinistral) from high latitudes: new paleoenvironmental insights, *Geo-Mar Lett*,



565 41, 2, <https://doi.org/10.1007/s00367-020-00677-1>, 2021.

Bradshaw, J. S.: Laboratory experiments on the ecology of foraminifera., Cushman Found Foram. Res., Contr., 12, 87–106, 1961.

Broecker, W. S. and Peng, T.-H.: Gas exchange rates between air and sea, Tellus A: Dynamic Meteorology and Oceanography, 26, 21-35, <https://doi.org/10.3402/tellusa.v26i1-2.9733>, 1974.

570 Burke, J. E., Renema, W., Schiebel, R., and Hull, P. M.: Three-dimensional analysis of inter-and intraspecific variation in ontogenetic growth trajectories of planktonic foraminifera, Marine Micropaleontology, 155, 101794, <https://doi.org/10.1016/j.marmicro.2019.101794>, 2020.

Burke, J. E., Elder, L. E., Maas, A. E., Gaskell, D. E., Clark, E. G., Hsiang, A. Y., Foster, G. L., and Hull, P. M.: Physiological and morphological scaling enables gigantism in pelagic protists, Limnology and Oceanography, 575 70, 461-476, <https://doi.org/10.1002/lno.12770>, 2025.

580 Cesbron, F., Geslin, E., Jorissen, F. J., Delgard, M. L., Charrieau, L., Deflandre, B., Jézéquel, D., Anschutz, P., and Metzger, E.: Vertical distribution and respiration rates of benthic foraminifera: Contribution to aerobic remineralization in intertidal mudflats covered by *Zostera noltei* meadows, Estuarine, Coastal and Shelf Science, 179, 23–38, <https://doi.org/10.1016/j.ecss.2015.12.005>, 2016.

Chaabane, S., de Garidel-Thoron, T., Meilland, J., Sulpis, O., Chalk, T. B., Brummer, G.-J. A., Mortyn, P. G., Giraud, X., Howa, H., Casajus, N., Kuroyanagi, A., Beaugrand, G., and Schiebel, R.: Migrating is not enough for modern planktonic foraminifera in a changing ocean, Nature, 636, 390–396, <https://doi.org/10.1038/s41586-024-08191-5>, 2024.

585 Coletti, G., Stainbank, S., Fabbrini, A., Spezzaferri, S., Foubert, A., Kroon, D., and Betzler, C.: Biostratigraphy of large benthic foraminifera from Hole U1468A (Maldives): a CT-scan taxonomic approach, Swiss J Geosci, 111, 523–536, <https://doi.org/10.1007/s00015-018-0306-7>, 2018.

Darling, K. F., Kucera, M., Pudsey, C. J., and Wade, C. M.: Molecular evidence links cryptic diversification in polar planktonic protists to Quaternary climate dynamics, Proceedings of the National Academy of Sciences, 590 101, 7657–7662, <https://doi.org/10.1073/pnas.0402401101>, 2004.

Darling, K. F., Kucera, M., Kroon, D., and Wade, C. M.: A resolution for the coiling direction paradox in *Neogloboquadrina pachyderma*, Paleoceanography, 21, PA2011, <https://doi.org/10.1029/2005PA001189>, 2006.

Darling, K. F., Kucera, M., and Wade, C. M.: Global molecular phylogeography reveals persistent Arctic circumpolar isolation in a marine planktonic protist, Proc. Natl. Acad. Sci. U.S.A., 104, 5002–5007, <https://doi.org/10.1073/pnas.0700520104>, 2007.

Davis, C. V., Rivest, E. B., Hill, T. M., Gaylord, B., Russell, A. D., and Sanford, E.: Ocean acidification compromises a planktic calcifier with implications for global carbon cycling, Scientific reports, 7, 2225,



<https://doi.org/10.1038/s41598-017-01530-9>, 2017.

600 de la Vega, E., Raitzsch, M., Foster, G., Bijma, J., Ninnemann, U.S., Kucera, M., Babilia, T.L., Crumpton Banks, J., Ezat, M.M. and Morley, A., 2025. A  $\delta$  11 B-pH calibration for the high-latitude foraminifera species *Neogloboquadrina pachyderma* and *Neogloboquadrina incompta*. *EGUsphere*, 2025, pp.1-32, <https://doi.org/10.5194/egusphere-2025-2443>

605 de Nooijer, L. J., Spero, H. J., Erez, J., Bijma, J., and Reichart, G. J.: Biomineralization in perforate foraminifera, *Earth-Science Reviews*, 135, 48–58, <https://doi.org/10.1016/j.earscirev.2014.03.013>, 2014.

610 DeLong, J. P., Okie, J. G., Moses, M. E., Sibly, R. M., and Brown, J. H.: Shifts in metabolic scaling, production, and efficiency across major evolutionary transitions of life, *Proceedings of the National Academy of Sciences*, 107, 12941–12945, <https://doi.org/10.1073/pnas.1007783107>, 2010.

615 Dickson, A. G. and Riley, J. P.: The estimation of acid dissociation constants in seawater media from potentiometric titrations with strong base. I. The ionic product of water —  $K_w$ , *Marine Chemistry*, 7, 89–99, [https://doi.org/10.1016/0304-4203\(79\)90001-X](https://doi.org/10.1016/0304-4203(79)90001-X), 1979.

620 Eggins, S. M., Sadekov, A., and De Deckker, P.: Modulation and daily banding of Mg/Ca in *Orbulina universa* tests by symbiont photosynthesis and respiration: a complication for seawater thermometry?, *Earth and Planetary Science Letters*, 225, 411–419, <https://doi.org/10.1016/j.epsl.2004.06.019>, 2004.

625 El Bani Altuna, N., Pieńkowski, A. J., Eynaud, F., and Thiessen, R.: The morphotypes of *Neogloboquadrina pachyderma*: Isotopic signature and distribution patterns in the Canadian Arctic Archipelago and adjacent regions, *Marine Micropaleontology*, 142, 13–24, <https://doi.org/10.1016/j.marmicro.2018.05.004>, 2018.

630 Fabbrini, A., Pearson, P. N., Brombacher, A., Iacoviello, F., Ezard, T. H., and Wade, B. S.: Morphology of *Pulleniatina* (planktonic foraminifera) from optical microscopy, micro-CT, and SEM investigations. *Journal of Micropalaeontology*, 44, 213–235, <https://doi.org/10.5194/jm-44-213-2025>, 2025.

635 Fabbrini, A., Meilland, J., Westgård, A., Sykes, F.E., Ezat, M.M., and Morley, A.: Extensive culturing experiment on *Turborotalita quinqueloba* (spinose planktonic foraminifera). *Journal of Plankton Research*, submitted.

640 Fenchel, T. and Finlay, B. J.: Respiration rates in heterotrophic, free-living protozoa, *Microbial Ecology*, 9, 99–122, <https://doi.org/10.1007/BF02015125>, 1983.

645 Gerlach, S. A., Hahn, A. E., and Schrage, M.: Size spectra of benthic biomass and metabolism, *Marine Ecology Progress Series*, 26, 161–173, <http://www.jstor.org/stable/24817617>, 1985.

650 Geslin, E., Risgaard-Petersen, N., Lombard, F., Metzger, E., Langlet, D., and Jorissen, F.: Oxygen respiration rates of benthic foraminifera as measured with oxygen microsensors, *Journal of Experimental Marine Biology and Ecology*, 396, 108–114, <https://doi.org/10.1016/j.jembe.2010.10.011>, 2011.



635 Glock, N., Romero, D., Roy, A. S., Woehle, C., Dale, A. W., Schönfeld, J., Wein, T., Weissenbach, J., and Dagan, T.: A hidden sedimentary phosphate pool inside benthic foraminifera from the Peruvian upwelling region might nucleate phosphogenesis, *Geochimica et Cosmochimica Acta*, 289, 14–32, <https://doi.org/10.1016/j.gca.2020.08.002>, 2020.

640 Glock, N., Richirt, J., Woehle, C., Algar, C., Armstrong, M., Eichner, D., Firrincieli, H., Makabe, A., Govindankutty Menon, A., Ishitani, Y., Hackl, T., Hubert-Huard, R., Kienast, M., Milker, Y., Mutzberg, A., Ni, S., Okada, S., Rakshit, S., Schmiedl, G., Steiner, Z., Tame, A., Zhang, Z., and Nomaki, H.: Widespread occurrence and relevance of phosphate storage in foraminifera, *Nature*, 638, 1000–1006, <https://doi.org/10.1038/s41586-024-08431-8>, 2025.

Greco, M., Jonkers, L., Kretschmer, K., Bijma, J., and Kucera, M.: Depth habitat of the planktonic foraminifera *Neogloboquadrina pachyderma* in the northern high latitudes explained by sea-ice and chlorophyll concentrations, *Biogeosciences*, 16, 3425–3437, <https://doi.org/10.5194/bg-16-3425-2019>, 2019.

645 Greco, M., Meilland, J., Zamelczyk, K., Rasmussen, T. L., and Kučera, M.: The effect of an experimental decrease in salinity on the viability of the Subarctic planktonic foraminifera *Neogloboquadrina incomppta*, *Polar Research*, 39, <https://doi.org/10.33265/polar.v39.3842>, 2020.

Hannah, F., Rogerson, R., and Laybourn-Parry, J.: Respiration rates and biovolumes of common benthic Foraminifera (Protozoa), *J. Mar. Biol. Ass.*, 74, 301–312, <https://doi.org/10.1017/S0025315400039345>, 1994.

650 Hemleben, C., Spindler, M., and Anderson, O. R.: Taxonomy and Species Features, in: *Modern Planktonic Foraminifera*, edited by: Hemleben, C., Spindler, M., and Anderson, O. R., Springer, New York, NY, 8–32, [https://doi.org/10.1007/978-1-4612-3544-6\\_2](https://doi.org/10.1007/978-1-4612-3544-6_2), 1989.

655 Hoogakker, B. A. A., Anderson, C., Paoloni, T., Stott, A., Grant, H., Keenan, P., Mahaffey, C., Blackbird, S., McClymont, E. L., Rickaby, R., Poulton, A., and Peck, V. L.: Planktonic foraminifera organic carbon isotopes as archives of upper ocean carbon cycling, *Nat Commun*, 13, 4841, <https://doi.org/10.1038/s41467-022-32480-0>, 2022.

Huber, R., Meggers, H., Baumann, K.-H., Raymo, M. E., and Henrich, R.: Shell size variation of the planktonic foraminifer *Neogloboquadrina pachyderma* sin. in the Norwegian–Greenland Sea during the last 1.3 Myrs: implications for paleoceanographic reconstructions, *Palaeogeography, Palaeoclimatology, Palaeoecology*, 160, 193–212, [https://doi.org/10.1016/S0031-0182\(00\)00066-3](https://doi.org/10.1016/S0031-0182(00)00066-3), 2000.

Husum, K. and Hald, M.: Arctic planktic foraminiferal assemblages: Implications for subsurface temperature reconstructions, *Marine Micropaleontology*, 96–97, 38–47, <https://doi.org/10.1016/j.marmicro.2012.07.001>, 2012.

665 Iwasaki, S., Kimoto, K., and Kucera, M.: Development of a Deep-Water Carbonate Ion Concentration Proxy Based on Preservation of Planktonic Foraminifera Shells Quantified by X-Ray CT Scanning, *Paleoceanography and Paleoclimatology*, 38, e2022PA004601, <https://doi.org/10.1029/2022PA004601>, 2023.



670 Kanbur, S.: Neglected small foraminifers of the Eastern Mediterranean and their paleoecological importance, Journal of Foraminiferal Research, 55, 218–232, <https://doi.org/10.61551/gsjfr.55.2.218>, 2025.

675 Kiss, P., Hudáčková, N., Titschack, J., Siccha, M. G. R., Heřmanová, Z., Silye, L., Ruman, A., Rybár, S., and Kučera, M.: Convergent evolution of spherical shells in Miocene planktonic foraminifera documents the parallel emergence of a complex character in response to environmental forcing, Paleobiology, 49, 454–470, <https://doi.org/10.1017/pab.2022.48>, 2023.

Kleiber, M.: Body size and metabolism, Hilgardia, 6, 315, 1932.

680 Köhler-Rink, S. and Kühl, M.: Microsensor studies of photosynthesis and respiration in the larger symbiont bearing foraminifera *Amphistegina lobifera*, and *Amphisorus hemprichii*, Ophelia, 55, 111–122, <https://doi.org/10.1080/00785236.2001.10409478>, 2001.

Kucera, M. and Kennett, J. P.: Causes and consequences of a middle Pleistocene origin of the modern planktonic foraminifer *Neogloboquadrina pachyderma* sinistral, Geology, 30, 539–542, [https://doi.org/10.1130/0091-7613\(2002\)030%3C0539:CACOAM%3E2.0.CO;2](https://doi.org/10.1130/0091-7613(2002)030%3C0539:CACOAM%3E2.0.CO;2), 2002.

685 Lewis, E. R. and Wallace, D. W. R.: Program developed for CO<sub>2</sub> system calculations, Environmental System Science Data Infrastructure for a Virtual Ecosystem, <https://doi.org/10.15485/1464255>, 1998.

Lombard, F., Erez, J., Michel, E., and Labeyrie, L.: Temperature effect on respiration and photosynthesis of the symbiont-bearing planktonic foraminifera *Globigerinoides ruber*, *Orbulina universa*, and *Globigerinella siphonifera*, Limnology and Oceanography, 54, 210–218, <https://doi.org/10.4319/lo.2009.54.1.0210>, 2009.

690 Lopes, A. S., Larsen, L. H., Ramsing, N., Løvendahl, P., Raty, M., Peippo, J., Greve, T., and Callesen, H.: Respiration rates of individual bovine in vitro-produced embryos measured with a novel, non-invasive and highly sensitive microsensor system, Reproduction, 130, 669–679, <https://doi.org/10.1530/rep.1.00703>, 2005.

695 Lucke, T. J., Dickson, A. G., and Keeling, C. D.: Ocean *p*CO<sub>2</sub> calculated from dissolved inorganic carbon, alkalinity, and equations for *K*1 and *K*2: validation based on laboratory measurements of CO<sub>2</sub> in gas and seawater at equilibrium, Marine Chemistry, 70, 105–119, [https://doi.org/10.1016/S0304-4203\(00\)00022-0](https://doi.org/10.1016/S0304-4203(00)00022-0), 2000.

Maciute, A., Holovachov, O., Glud, R. N., Broman, E., Berg, P., Nascimento, F. J. A., and Bonaglia, S.: Reconciling the importance of meiofauna respiration for oxygen demand in muddy coastal sediments, Limnology and Oceanography, 68, 1895–1905, <https://doi.org/10.1002/lno.12393>, 2023.

700 Manno, C., Morata, N., and Bellerby, R.: Effect of ocean acidification and temperature increase on the planktonic foraminifer *Neogloboquadrina pachyderma* (sinistral), Polar Biol, 35, 1311–1319, <https://doi.org/10.1007/s00300-012-1174-7>, 2012.



Meiland, J., Howa, H., Hulot, V., Demangel, I., Salaün, J., and Garlan, T.: Population dynamics of modern planktonic foraminifera in the western Barents Sea, *Biogeosciences*, <https://doi.org/10.5194/bg-2019-429>, 2019.

Moens, T., Verbeeck, L., and Vincx, M.: Feeding biology of a predatory and a facultatively predatory nematode (*Enoploides longispiculosus* and *Adoncholaimus fuscus*), *Marine Biology*, 134, 585–593, <https://doi.org/10.1007/s002270050573>, 1999.

Moodley: Biomass-specific respiration rates of benthic meiofauna: Demonstrating a novel oxygen micro-respiration system, *Journal of Experimental Marine Biology and Ecology*, 357, 41–47, <https://doi.org/10.1016/j.jembe.2007.12.025>, 2008.

710 Motic Instruments Inc: <https://moticeurope.com/en/moticam-x5-plus.html>, 2024.

Mundim, K.C., Baraldi, S., Machado, H.G. and Vieira, F.M. Temperature coefficient (Q10) and its applications in biological systems: Beyond the Arrhenius theory. *Ecol Model.*, 431, 109127. 2020.

715 Natland, M. L.: New species of foraminifera from off the West Coast of North America and from the later Tertiary of the Los Angeles basin, University of California Press, [New species of foraminifera from off the West Coast of North America and from the later Tertiary of the Los Angeles basin | CiNii Research](#), 1938.

Nielsen, P., Larsen, L. H., Ramløv, H., and Hansen, B. W.: Respiration rates of subitaneous eggs from a marine calanoid copepod: monitored by nanorespirometry, *Journal of Comparative Physiology B*, 177, 287–296, <https://doi.org/10.1007/s00360-006-0128-1>, 2007.

720 Nomaki, H., Yamaoka, A., Shirayama, Y., and Kitazato, H.: Deep-sea benthic foraminiferal respiration rates measured under laboratory conditions, *Journal of Foraminiferal Research*, 37, 281–286, <https://doi.org/10.2113/gsjfr.37.4.281>, 2007.

725 Pearson, P.N. and Kucrea, M. Taxonomy, biostratigraphy, and phylogeny of Oligocene Turborotalita, in Wade, B.S., Olsson, R.K., Pearson, P.N., Huber, B.T. and Berggren, W.A. (eds.), *Atlas of Oligocene Planktonic Foraminifera*, Cushman Foundation of Foraminiferal Research, Special Publication, No. 46: [https://www.ucl.ac.uk/earth-sciences/sites/earth\\_sciences/files/Chapter\\_12.pdf](https://www.ucl.ac.uk/earth-sciences/sites/earth_sciences/files/Chapter_12.pdf), 2018.

730 Pérez-Huerta, A. and Andrus, C. F. T.: Vital effects in the context of biomineralization, *Seminarios de la Sociedad de Española de Mineralogía*, 7, 35–45, [ir-api.ua.edu/api/core/bitstreams/efc0bd9b-7204-464d-84b7-454793f7c34a/content](https://ir-api.ua.edu/api/core/bitstreams/efc0bd9b-7204-464d-84b7-454793f7c34a/content), 2010.

Rantanen, M., Karpechko, A. Y., Lipponen, A., Nordling, K., Hyvärinen, O., Ruosteenja, K., Vihma, T., and Laaksonen, A.: The Arctic has warmed nearly four times faster than the globe since 1979, *Commun Earth Environ*, 3, 168, <https://doi.org/10.1038/s43247-022-00498-3>, 2022.

735 Revsbech, N. P.: An oxygen microsensor with a guard cathode, *Limnology and Oceanography*, 34, 474–478,



<https://doi.org/10.4319/lo.1989.34.2.0474>, 1989.

Rink, S., Kühl, M., Bijma, J., and Spero, H. J.: Microsensor studies of photosynthesis and respiration in the symbiotic foraminifer *Orbulina universa*, *Marine Biology*, 131, 583–595,

740 740 <https://doi.org/10.1007/s002270050350>, 1998.

Schiebel, R., Waniek, J., Bork, M., and Hemleben, C.: Planktic foraminiferal production stimulated by chlorophyll redistribution and entrainment of nutrients, *Deep Sea Research Part I: Oceanographic Research Papers*, 48, 721–740, [https://doi.org/10.1016/S0967-0637\(00\)00065-0](https://doi.org/10.1016/S0967-0637(00)00065-0), 2001.

745 745 Schiebel, R. and Hemleben, C.: *Planktic Foraminifers in the Modern Ocean*, Springer Berlin / Heidelberg, Berlin, Heidelberg, Germany, 2017.

Schlitzer, R.: Ocean data view, <https://odv.awi.de>, last access: 1 September 2025, 2022.

750 750 Schmidt-Nielsen, K.: *Animal Physiology: Adaptation and Environment*, Cambridge University Press, 630 pp., 1997.

Serreze, M. C. and Barry, R. G.: Processes and impacts of Arctic amplification: A research synthesis, *Global and Planetary Change*, 77, 85–96, <https://doi.org/10.1016/j.gloplacha.2011.03.004>, 2011.

755 755 Siccha, M., Morard, R., Meilland, J., Iwasaki, S., Kucera, M., and Kimoto, K.: Collection of X-ray micro computed tomography images of shells of planktic foraminifera with curated taxonomy, *Sci Data*, 10, 679, <https://doi.org/10.1038/s41597-023-02498-0>, 2023.

760 760 Spero, H. J. and Lea, D. W.: Intraspecific stable isotope variability in the planktic foraminifera *Globigerinoides sacculifer*: Results from laboratory experiments, *Marine Micropaleontology*, 22, 221–234, [https://doi.org/10.1016/0377-8398\(93\)90045-Y](https://doi.org/10.1016/0377-8398(93)90045-Y), 1993.

Spero, H. J. and Lea, D. W.: Experimental determination of stable isotope variability in *Globigerina bulloides*: implications for paleoceanographic reconstructions, *Marine Micropaleontology*, 28, 231–246, [https://doi.org/10.1016/0377-8398\(96\)00003-5](https://doi.org/10.1016/0377-8398(96)00003-5), 1996.

765 765 Spindler M.: On the salinity tolerance if the planktonic foraminifer *Neogloboquadrina pachyderma* from the Antarctic Sea Ice (17th Symposium on Polar Biology), *Proceedings of the NIPR Symposium on Polar Biology*, 9, 85–91, <https://doi.org/10.15094/00005306>, 1996.

Spindler, M. and Dieckmann, G. S.: Distribution and abundance of the planktic foraminifer *Neogloboquadrina pachyderma* in sea ice of the Weddell Sea (Antarctica), *Polar Biol*, 5, 185–191,

770 770 <https://doi.org/10.1007/BF00441699>, 1986.

Stalling, D., Westerhoff, M., and Hege, H.-C.: Amira: A Highly Interactive System for Visual Data Analysis, in:



Visualization Handbook, Elsevier, 749–767, <https://doi.org/10.1016/B978-012387582-2/50040-X>, 2005.

Stangeew, E.: Distribution and Isotopic Composition of Living Planktonic Foraminifera *N. pachyderma* (sinistral) and *T. quinqueloba* in the High Latitude North Atlantic, Kiel, University, Diss., 2001.

775

Takagi, H., Kimoto, K., Fujiki, T., Saito, H., Schmidt, C., Kucera, M., and Moriya, K.: Characterizing photosymbiosis in modern planktonic foraminifera, Biogeosciences, 16, 3377–3396, <https://doi.org/10.5194/bg-16-3377-2019>, 2019.

780

Tell, F., Jonkers, L., Meiland, J., and Kucera, M.: Upper-ocean flux of biogenic calcite produced by the Arctic planktonic foraminifera *Neogloboquadrina pachyderma*, Biogeosciences, 19, 4903–4927, <https://doi.org/10.5194/bg-19-4903-2022>, 2022.

785

Titschack, J., Baum, D., Matsuyama, K., Boos, K., Färber, C., Kahl, W.-A., Ehrig, K., Meinel, D., Soriano, C., and Stock, S. R.: Ambient occlusion – A powerful algorithm to segment shell and skeletal intrapores in computed tomography data, Computers & Geosciences, 115, 75–87, <https://doi.org/10.1016/j.cageo.2018.03.007>, 2018.

Unisense.: Nanorespiration system manual.

790

[tawk.link/61939a4d6885f60a50bc0657/a/61dc3217009bc10c82950cbd/abf1e839a61c637794a6fcc88a0563558996bd94/Nanorespiration\\_system\\_manual\\_www.pdf](tawk.link/61939a4d6885f60a50bc0657/a/61dc3217009bc10c82950cbd/abf1e839a61c637794a6fcc88a0563558996bd94/Nanorespiration_system_manual_www.pdf), 2025.

Volkmann, R.: Planktic foraminifers in the outer Laptev Sea and the Fram Strait- Modern distribution and ecology, Journal of Foraminiferal Research, 30, 157–176, <https://doi.org/10.2113/0300157>, 2000.

795

Westgård, A., Ezat, M. M., Chalk, T. B., Chierici, M., Foster, G. L., and Meiland, J.: Large-scale culturing of *Neogloboquadrina pachyderma*, its growth in, and tolerance of, variable environmental conditions, Journal of Plankton Research, 45, 732–745, <https://doi.org/10.1093/plankt/fbad034>, 2023.

800

Wieser, W.: Temperature Relations of Ectotherms: A Speculative Review, in: Effects of Temperature on Ectothermic Organisms, edited by: Wieser, W., Springer Berlin Heidelberg, Berlin, Heidelberg, 1–23, [https://doi.org/10.1007/978-3-642-65703-0\\_1](https://doi.org/10.1007/978-3-642-65703-0_1), 1973.

Woelfel, J., Sørensen, K., Warkentin, M., Forster, S., Oren, A., and Schumann, R.: Oxygen evolution in a hypersaline crust: in situ photosynthesis quantification by microelectrode profiling and use of planar optode spots in incubation chambers, Aquat. Microb. Ecol., 56, 263–273, <https://doi.org/10.3354/ame01326>, 2009.

805

Wolf-Gladrow, D. A., Bijma, J., and Zeebe, R. E.: Model simulation of the carbonate chemistry in the microenvironment of symbiont bearing foraminifera, Marine Chemistry, 64, 181–198, [https://doi.org/10.1016/S0304-4203\(98\)00074-7](https://doi.org/10.1016/S0304-4203(98)00074-7), 1999.

Ying, R., Monteiro, F. M., Wilson, J. D., and Schmidt, D. N.: ForamEcoGENIE 2.0: incorporating symbiosis and



spine traits into a trait-based global planktic foraminiferal model, *Geosci. Model Dev.*, 16, 813–832,  
<https://doi.org/10.5194/gmd-16-813-2023>, 2023.

810

Zamelczyk, K., Fransson, A., Chierici, M., Jones, E., Meiland, J., Anglada-Ortiz, G., and Lødlemel, H. H.:  
Distribution and Abundances of Planktic Foraminifera and Shelled Pteropods During the Polar Night in the Sea-  
Ice Covered Northern Barents Sea, *Front. Mar. Sci.*, 8, <https://doi.org/10.3389/fmars.2021.644094>, 2021.

815 Zeebe, R. E. and Sanyal, A.: Comparison of two potential strategies of planktonic foraminifera for house  
building: Mg<sup>2+</sup> or H<sup>+</sup> removal?, *Geochimica et Cosmochimica Acta*, 66, 1159–1169,  
[https://doi.org/10.1016/S0016-7037\(01\)00852-3](https://doi.org/10.1016/S0016-7037(01)00852-3), 2002.

ZEISS. Xradia VERSA 620 User Manual. [www.zeiss.com](http://www.zeiss.com). 2024.

820